High-power cw bismuth-fiber lasers

Evgeny M. Dianov, Alexey V. Shubin, Mikhail A. Melkumov, Oleg I. Medvedkov, and Igor A. Bufetov*

Fiber Optics Research Center of the Russian Academy of Sciences, 38 Vavilov Street, 119333 Moscow, Russia
**Corresponding author: iabuf@fo.gpi.ru*

Received October 2, 2006; accepted November 7, 2006;
posted November 27, 2006 (Doc. ID 75675); published July 19, 2007

Continuous-wave lasing of Bi-doped fiber lasers in a wavelength range of 1150–1215 nm with a power of up to 15 W has been obtained for the first time. The unsaturable optical losses in Bi-doped fibers have been revealed and their influence on the Bi-laser operation is investigated. Frequency doubling of the Bi-fiber laser radiation is demonstrated that can be used as a yellow light source (wavelength of 580 nm). © 2007 Optical Society of America

OCIS codes: 140.3380, 140.3510, 060.2320.

1. INTRODUCTION

In the past two decades highly effective fiber lasers with rare-earth ions Yb^{3+}, Er^{3+}, Nd^{3+}, and Tm^{3+} as active centers in silica-based fibers have been developed. The working wavelength bands of these lasers are situated in the region 0.9–2.1 μm with large spectral gaps between them. Generally speaking, Raman fiber lasers can be used at wavelengths not covered by rare-earth lasers [1]. However, Raman fiber lasers have their own drawbacks associated with inevitable high nonlinearity of the active fiber and limitations in the pulse-mode operation. Thus, search for and investigation of new fiber laser media covering the wavelength intervals between rare-earth fiber lasers is of interest.

Efficient solid-state (fiber) laser sources for a spectral region of 1150–1500 nm are becoming now indispensable for numerous applications. The forecast of optical fiber communications progress for the next two decades suggests that all spectral range between 1300 and 1700 nm will be used for transmission [2]. However, there are no efficient silica-based fiber lasers and wideband optical amplifiers operating between 1300 and 1500 nm, which are required for optical communications systems. Therefore, such devices must be developed.

The creation of efficient lasers generating between 1150 and 1500 nm will allow construction of efficient visible lasers, in particular yellow-light sources, by frequency doubling. It is known that the 570–580 nm band is very promising for ophthalmology and dermatology applications (e.g. [3,4]). Besides, there is a need for a high-brightness 589 nm source to generate laser guide stars for adaptive optics corrector of large telescopes [5]. To have efficient, compact, and reliable sources in the region 1150–1500 nm, it is desirable to develop a solid-state or fiber laser generating directly in this spectral region.

Recently, observation of a broadband luminescence in the near-IR region (1100–1700 nm) in a number of Bi-doped glasses (silicate, germanate, aluminophosphate, barium-aluminoborate) has been reported [6–9]. The nature of the active center is still unclear; it has been attributed to Bi^{+} as well as to Bi^{5+} or even to Bi clusters, but apparently the luminescence takes place only in the presence of Al or Ta. For brevity, below, these active centers will be referred to as "Bi ions." The broadband luminescence of Bi-doped glasses enables one to consider different versions of these glasses as possible active media for lasers in the wavelength range of 1100–1700 nm. Recently, the first fabrication of Bi-doped aluminosilicate fibers by the modified-chemical-vapor deposition (MCVD) technique and preliminary results on laser action in these fibers in the range of 1150–1300 nm by pumping at 1064 nm with a Nd:YAG laser were reported [10,11].

In this paper, we report new results on the development of a cw 10 W-level all-fiber Bi-doped laser and frequency doubling of its output radiation.

2. EXPERIMENTAL SETUP

The scheme of the experiment is shown in Fig. 1. As a source of pump radiation, a cw Yb fiber laser based on phosphosilicate fiber was used. The output power of this laser was up to 80 W at the wavelength of 1070 nm. In some experiments, a laser with a lower power at the wavelength of 1085 nm was used.

A single-mode Bi-doped fiber with a cutoff wavelength of ~1.1 μm (the core-cladding index difference of $\approx 5 \times 10^{-3}$) was used as an active medium. The fiber was drawn from a preform fabricated by the MCVD technique. The mode field diameter at 1.1 μm was 6.8 μm. The concentration of Bi in the aluminosilicate glass of the core did not exceed 2×10^{-2} at. % (in other words, less than $1.3 \times 10^{19} \mathrm{cm}^{-3}$) [12].

The absorption spectrum of this fiber in the spectral region 1000–1700 nm is shown in Fig. 2. The absorption band with a maximum near 1000 nm and a long wavelength edge near 1200 nm corresponds to Bi-ion absorption. It is necessary to note that optical losses at the wavelength band at about 1300 nm are less than 10 dB/km. This means that background losses in the Bi-doped fiber under investigation are no larger than this value. Absorption of the pump radiation is equal to 0.29 dB/m for 1070 nm and 0.26 dB/m for 1085 nm. For

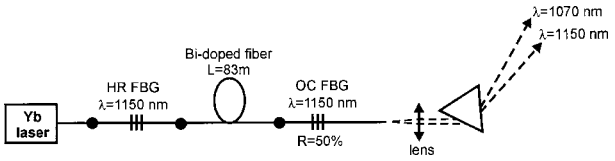

Fig. 1. Scheme of a Bi-doped fiber laser.

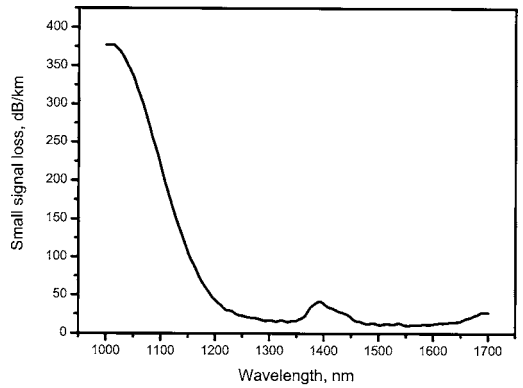

Fig. 2. Optical-loss spectrum of a Bi-doped fiber. Loss increase in the vicinity of 1400 nm is due to presence of OH groups.

this reason, the length of the fiber $L=(50-80)$ m used in Bi-laser schemes was long enough for efficient pump radiation absorption.

The position, shape, and amplitude of the Bi ions luminescence band depend, in general, on the pump wavelength. Figure 3 shows the luminescence spectra of Bi-doped aluminosilicate glass under the action of the same pump power at three different pump wavelengths λ_p. If λ_p is near 1 μm, a single luminescence band of Bi-doped glass with a maximum at about 1.15 μm is observed. However, if the pump wavelength is shorter (λ_p =877 nm), two different luminescence bands (1 and 2, Fig. 3) arise. These two luminescence bands are characterized, apparently, by different lifetimes: ≈800 μs for band 1 and less than 20 μs (the time resolution of the measuring equipment) [12] for band 2.

The cavity of the Bi-fiber laser was formed by two fiber Bragg gratings (FBGs). FBGs were written in sections of special photosensitive Ge-doped fibers and then spliced with the Bi-doped fiber. The output coupler (OC) FBG has a reflectivity $R\approx 50\%$ in most experiments. The spectral

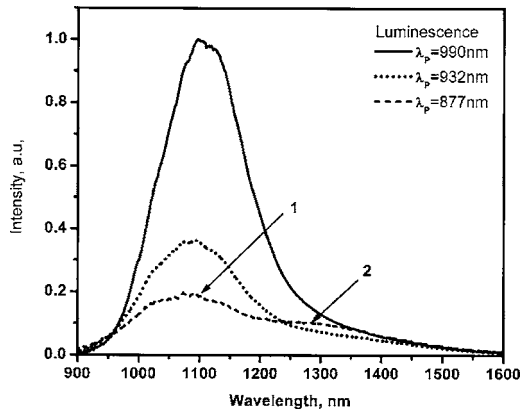

Fig. 3. Luminescence spectra of Bi-doped aluminosilicate glass with a Bi concentration of 0.15 at. %.

width of the FBG was ≈1 nm, except for the experiments on yellow-light generation. A dispersing prism was used for separation of the pump and Bi-laser radiation at the output of the Bi-laser.

3. EXPERIMENTAL RESULTS

A. Output Parameters of cw Bi Lasers

At the output of the laser scheme (Fig. 1), the radiation of the Bi-fiber laser and unabsorbed pump radiation were observed. Figure 4 shows the dependences of the unabsorbed pump power P_{up} and the laser radiation power P_{Bi} on the pump power (P_{in}) launched into the Bi-laser fiber for four Bi lasers at wavelengths of 1150, 1160, 1205, and 1215 nm. The Bi-doped fiber length was in each case equal to $L\approx 80$ m.

The Bi-fiber lasers at 1150 and 1160 nm demonstrated the maximal efficiency of 19% and 21%, respectively, and the maximal output power of 13 and 15 W, respectively. Most of the pump radiation in all the four lasers was absorbed in the Bi-doped fiber. The longer the lasing wavelength in the region of 1150–1205 nm, the lower the efficiency of the Bi-fiber laser. Up to the wavelength of 1205 nm the $P_{Bi}(P_{in})$ dependence remains close to a linear one. Already in 10 nm (at $\lambda_s=1215$ nm) the $P_{Bi}(P_{in})$ dependence changes drastically; the saturation of the output power of the Bi laser is observed (see Fig. 4d). Simultaneously an increase of the unabsorbed pump power takes place. The initial slope efficiency of the 1215 nm laser ($P_{in}<15$ W) is higher than that of 1205 nm laser. In addition, Raman Stokes generation starts in the Bi-fiber laser ($\lambda_s=1215$ nm) at a pump higher than 60 W, which results in an abrupt reduction of the unabsorbed pump power and Bi-laser radiation. The spectrum of the output radiation in this case is shown in Fig. 5.

The left spectral band in Fig. 5 is the pump radiation at the wavelength $\lambda_p=1070$ nm. The central band has a two-maxima structure, which is a characteristic feature of the Raman spectrum in silica. The frequency shift between

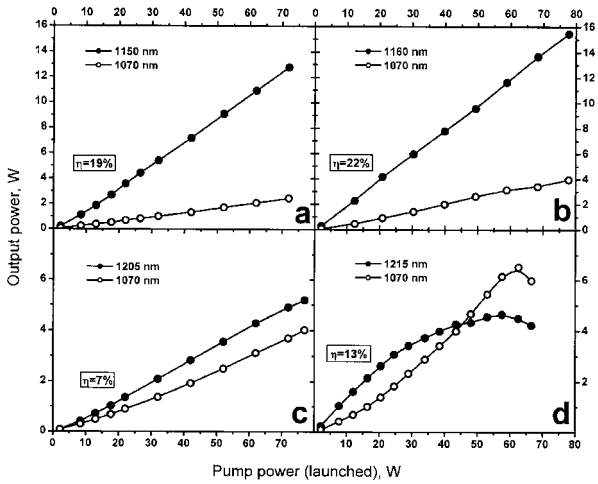

Fig. 4. Variation of the radiation power at the output of the Bi-fiber laser with pump power ($\lambda_p\approx 1070$ nm) launched into a Bi-doped fiber for different lasing wavelengths (room temperature). η is the average slope efficiency (a, b, and c) and a slope efficiency for a pump power less than 15 W (d) with respect to absorbed pump power.

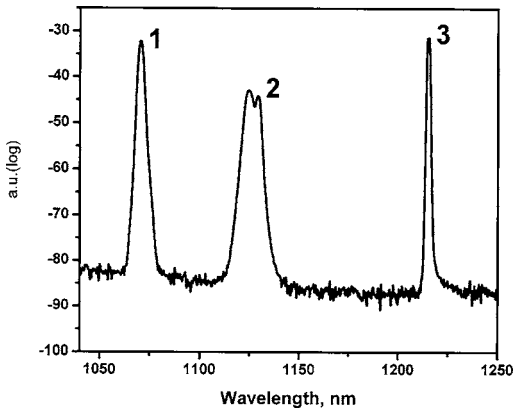

Fig. 5. Output spectrum of the Bi-fiber laser, $P_{in}=65$ W, $\lambda_s=1215$ nm, $L=78$ m. 1, unabsorbed pump radiation; 2, Raman lasing; 3, Bi laser output radiation.

the pump band and the maxima of the central band is 452 and 490 cm^{-1}, which agree satisfactorily with the main Raman shifts in silica (440 and 490 cm^{-1}). The cavity for Raman generation is formed apparently by two cleaved fiber ends at the output of the Bi-laser and before the highly reflective (HR) FBG of the Yb fiber laser. The spectrum line at 1215 nm in Fig. 5 is the Bi-laser radiation.

B. Temperature Dependence of Lasing

In all the experiments described above, the Bi-doped fiber was initially at room temperature ($T\approx25°C$). The Bi-doped fiber was wound on a thin-wall aluminum spool with a low heat capacity, so that all the fiber length was in contact with the aluminum surface. The spool was used as a heat sink for the Bi-doped fiber. In the experiments with a high pump power, we observed a temperature increase of the fiber and of the spool by $\approx10-20°C$. We then measured the dependence of the output power of the Bi laser on the fiber temperature in the range of $0-60°C$. For this experiment, the fiber was rewound on another, high-heat-capacity, temperature-controlled spool providing a good heat contact between the fiber and the spool. One of the Bi-fiber laser output power dependences on the fiber temperature is shown in Fig. 6.

This dependence is nearly linear and shows a ≈40% reduction of the output power with a temperature increase from 0 to 60°C. Figure 7 shows the experimental dependences of the output power and the unabsorbed pump power on the pump power for two different conditions: (**a**) the Bi-doped fiber is placed on a low heat capacity spool at room temperature without temperature control and (**b**) the Bi-doped fiber is placed at 2°C on the high-heat-capacity spool with temperature control. Comparison of these dependences shows that at the lower temperature the laser power increases, and in the case of temperature stabilization the $P_{Bi}(P_{in})$ dependence is closer to a linear one than in case (**a**). In case (**a**), the temperature of the fiber grows at high pump powers that results in a reduction of the differential efficiency of the laser.

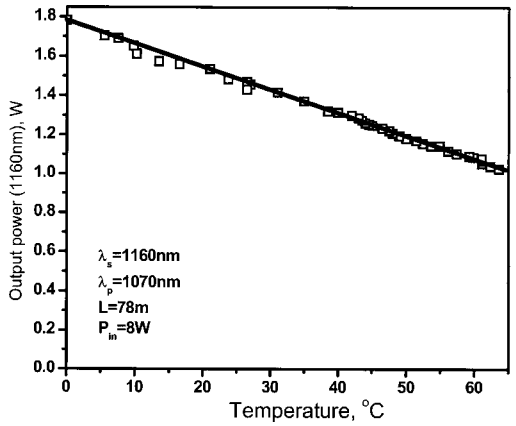

Fig. 6. Output power of the Bi-fiber laser against the fiber temperature at the pump power of 8 W.

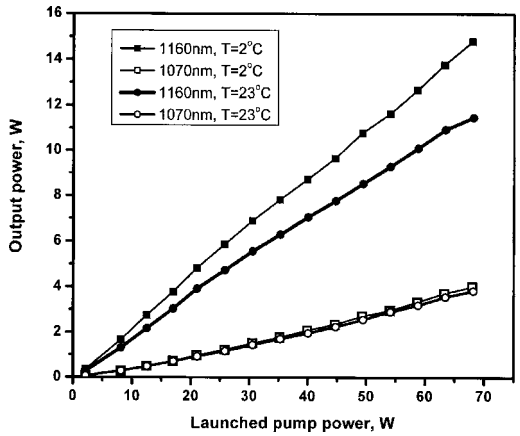

Fig. 7. $P_{Bi}(P_{in})$ and $P_{up}(P_{in})$ for Bi-fiber laser at 2°C and 23°C.

It is of interest to compare the behavior of the Bi-fiber lasers at 1160 and 1215 nm at different temperatures. Figure 8 shows that saturation of the output power of the 1215 nm Bi-fiber laser takes place at all three temperatures. For the Bi laser at the wavelength of 1215 nm, Fig. 8 indicates qualitatively the same dependences for the Bi-laser power on fiber temperature as Fig. 7 for the laser at 1160 nm. However, Fig. 8 shows a much stronger dependence of unabsorbed pump power on temperature than that for the laser at 1160 nm (see Fig. 7). The partial bleaching of the Bi-fiber at the pump wavelength of 1070 nm during lasing at 1215 nm occurs at a lower pump power at 4°C and at a higher pump power at 52°C. As a result, the Raman generation at 1125 nm is not observed at 52°C in the entire range of pump powers, in contrast

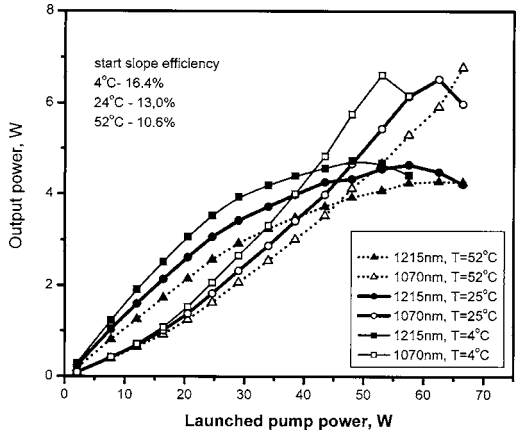

Fig. 8. $P_{Bi}(P_{in})$ and $P_{up}(P_{in})$ for the Bi-fiber laser with saturation of output power for different temperatures.

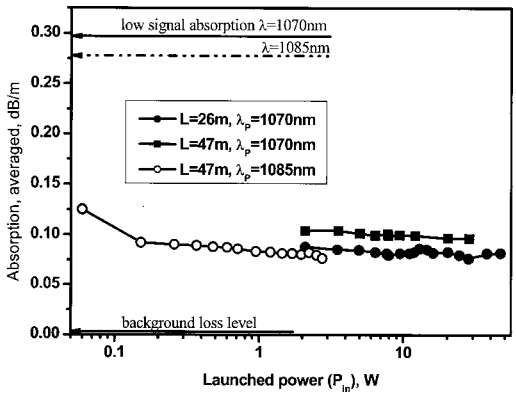

Fig. 9. Averaged optical losses of the Bi-doped fiber against launched power at room temperature.

with experiments with the same Bi-laser at 4°C and 25°C. The initial slope efficiency of the Bi-fiber laser (1215 nm) goes down with increasing the temperature, from 16.3% at 4°C to 10.6% at 52°C.

C. Unbleachable Optical Losses of Bi-Doped Fibers

The measured values of the Bi-lasers efficiency are essentially lower than, e.g., the efficiencies of widely used Yb- or Nd-fiber lasers. To find the mechanism of energy loss, we measured the absorption of pump radiation in the Bi-doped fiber. The experimental scheme used was similar to the scheme of Bi-laser shown in Fig. 1, but both FBGs were excluded. The measurements on Bi-doped fiber spans, 26 and 47 m in length, using the pump wavelengths of 1070 and 1085 nm, showed that there was an unsaturable absorption even for high input powers (up to 50 W, i.e., much higher than the saturation power of ~10 mW). In the entire range of pump powers, we did not observe any lasing effects in these experiments. The results of these measurements are shown in Fig. 9. It is possible to suppose that the origin of unsaturable optical losses is a very small excited-state lifetime of some share of Bi ions. In such a case this share amounts approximately to one-third of all the Bi ions in the fiber core. The presence of unsaturable optical losses, ~100 dB/km in magnitude, can explain the observed value of Bi-laser efficiency.

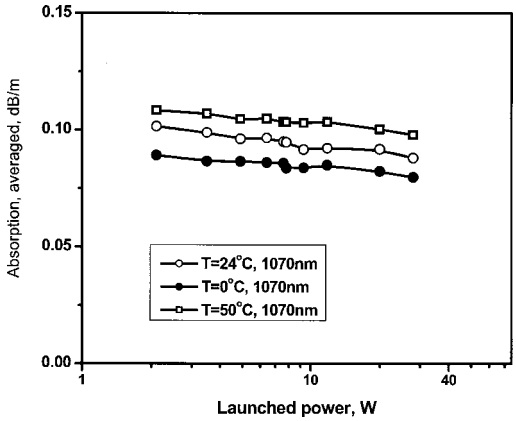

Fig. 10. Averaged optical losses of one and the same Bi-doped fiber against launched power at different temperatures.

The unsaturable losses in the Bi-doped fiber proved to depend on the temperature of the fiber. We measured the value of these losses using a 47 m fiber span. The measurements of the pump-power transmission were carried out at temperatures of 0, 24 and 50°C. During the measurements, the fiber was temperature stabilized. The results obtained are shown in Fig. 10. The observed dependence of the unsaturable optical losses in the Bi-doped fiber is in accordance with the temperature dependence of the laser output power.

4. YELLOW LIGHT GENERATION USING SECOND-HARMONIC GENERATION OF BI-FIBER LASER

The most effective 1160 nm Bi-fiber laser was used to demonstrate the possibility of yellow-light generation using frequency doubling of the cw Bi laser radiation. For this aim, we used a commercial 30 mm long periodically poled lithium niobate crystal with a fiber input (Global Fiberoptics, Ltd.). The expected efficiency of second-harmonic generation (SHG) (λ=580 nm) was ≈20% at 5 W linear polarized laser radiation with a wavelength bandwidth of less than 0.05 nm. The output radiation of all our Bi-fiber lasers was nonpolarized. For this reason, we were able to use no more than a half of the laser power for frequency doubling. The next question was the band-

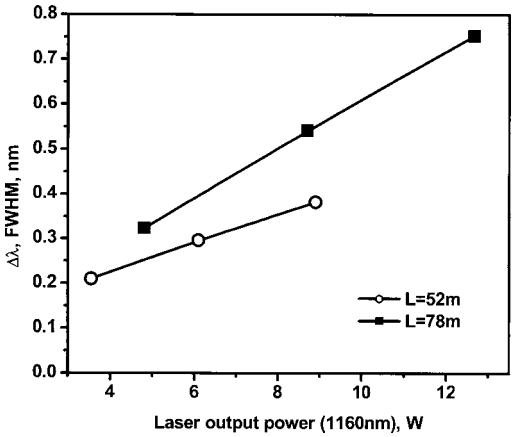

Fig. 11. Bandwidth of the Bi-laser radiation versus the output power of the Bi-laser.

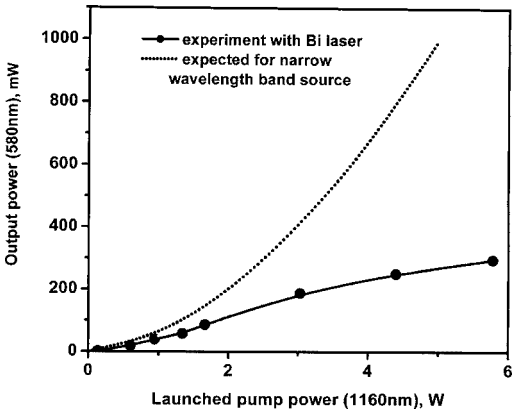

Fig. 12. Experimental dependence of the yellow-light output power versus the power of the Bi-fiber laser (one polarization).

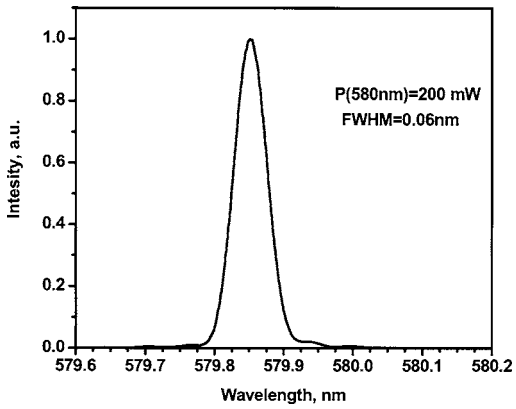

Fig. 13. Output spectrum of yellow light.

width of the Bi laser. To reduce the laser bandwidth, we used narrow FBGs (HR and OC) with a spectral width of ≈0.1 nm. However, owing to a low concentration of Bi ions in the fiber core, the length of the active fiber was sufficiently long enough ($L=78$ m). Under these conditions nonlinear processes, such as four-photon mixing, result in broadening of the laser spectrum, and the bandwidth of the spectrum depends on the fiber length and on the output power of the laser. The data obtained in our experiments with lasers 52 and 78 m in length are shown in Fig. 11. The efficiency of the cw SHG observed can be estimated using Fig. 12. It turns out to be about 5% with respect to one linearly polarized component of the Bi-laser output, or 2.5% with respect to the total output power. The maximal yellow cw radiation power obtained in our experiments was 300 mW. The output spectrum of yellow light is shown in Fig. 13.

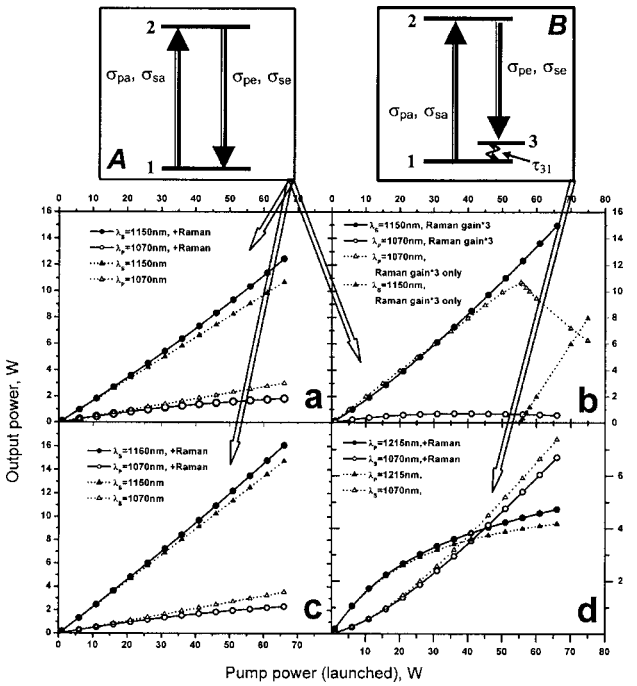

Fig. 14. Output powers of Bi-fiber lasers at the lasing and pump wavelengths calculated for different conditions. Graphs a, c, and d show results of real Bi laser scheme simulation for different wavelengths with (+Raman) and without regard to the Raman gain of the Bi-doped fiber. Graph b illustrates the output dependences of the Bi laser with three-times-higher Raman fiber gain than that for real conditions (solid curves) and (for comparison) output dependences in the same case but without amplification owing to the stimulated emission of Bi ions. Inset ***A*** shows the energy level scheme used for laser simulation at graphs a–c; the scheme shown in inset ***B*** was used for Bi laser simulation at 1215 nm (graph d).

5. DISCUSSION

The experimental results obtained were compared with the results of computer simulation of the Bi-fiber laser operation. The simulation was based on the following assumptions:

(a) An absorption band of a Bi ion with the center at about 1000 nm (Fig. 2) and a luminescence band with the center at about 1100 nm (Fig. 3) are due to the transitions between Bi ions energy levels joined into two energy bands (labeled **1** and **2** in Fig. 14, inset ***A***).

(b) transitions between bands **1** and **2** can be described in terms of wavelength-dependent emission and absorption cross sections (emission cross sections σ_{pe} and σ_{se} for pump and signal wavelengths and absorption cross-sections σ_{pa}, σ_{sa}, correspondingly) in a way used, e.g., in [13] with respect to Yb^{3+} ions in a glass.

As the first approximation for parameters of Bi ions (absorption and emission cross sections, lifetime, concentration) we used the data published in [14]. It turned out that satisfactory agreement between the experimental and calculated output power for the Bi-fiber laser at 1150, 1160, and 1205 nm can be achieved only by taking into account the unsaturable optical loss at the pump wavelength of the order of 100 dB/km (compare Figs. 4a and 4b with Figs. 14a and 14c, correspondingly). Moreover, for the same reason, it is necessary to use the Bi-ion concentration $\sim 10^{17}$ cm^{-3} for calculations. However, the simplest scheme of laser energy levels (Fig. 14, inset ***A***) cannot describe the phenomenon of output power saturation (see Fig. 14d and Fig. 8). Saturation can be taken into account using a more-complicated level scheme shown in Fig. 14, inset ***B*** with an additional third energy level (**3**) with a comparatively long relaxation time $\tau_{31} \sim 1$ μs between levels **3** and **1**. One more mechanism that can influence the process of lasing is Raman amplification. Obviously, for low-loss fibers ($\sim$1 dB/km), $\sim$100 m in length and for a single-mode pump power of tens of watts, Raman amplification can give rise to the laser generation in the cavity formed by cleaved fiber ends. However, the influence of Raman amplification on the Bi-fiber lasers investigated is suppressed: 1) by the additional optical losses in the fiber at the wavelength of interest and 2) by the fact that the frequency shift between the pump radiation and Bi lasing does not correspond to the maximal value of Raman gain. Thus, if the pump wavelength is 1070 nm, the frequency shift to 1150 nm is equal to 650 cm^{-1} and Raman gain can be estimated using the Raman spectrum of silica, the main constituent of the fiber core. The estimation is 0.127 with respect to the maximal Raman gain corresponding to the Raman shift of 440 cm^{-1}. For the other three lasing wavelengths, we have lasing at 1160 nm→frequency shift of 725 cm^{-1}→ Raman gain of 0.076; 1205 nm →1047 cm^{-1}→0.067; 1215 nm→1115 cm^{-1}→0.02. The

maximal value of the Bi-doped fiber Raman gain was estimated as ≈5 dB/(km·W). We included Raman amplification into the equations describing the process of light generation in the Bi laser. The results of numerical simulation with and without Raman gain are shown in Fig. 14. Figure 14a shows the calculated dependencies of $P_{Bi}(P_{in})$ and $P_{up}(P_{in})$ for the Bi-fiber laser with $L=78$ m and $\lambda_S=1150$ nm with and without regard to Raman gain. The curves obtained are in a satisfactory agreement with the dependence in Fig. 4a. It is seen that the addition of Raman amplification leads to saturation of the unabsorbed power dependence. Simultaneously there is a ~10% increase of the output power of the laser. Direct comparison of Figs. 4a and 14a allows one to conclude that the experimental output dependences are closer to the calculated dependences obtained without taking into account the Raman amplification. If we suppose that the fiber Raman gain is three times higher than that for real conditions corresponding to the dependences in Fig. 14a, we obtain two curves in Fig. 14b designated as "Raman gain*3." Thus, the essential increase of Raman component gives virtually no qualitative variation of the output dependences. The consequence is just a ~20% increase of the output power and saturation with decreasing the maximal value of the unabsorbed pump power. At the same time, if we rule out the gain due to stimulated emission of Bi ions, we obtain a quite different picture, typical of pure Raman lasers (Fig. 14b, "Raman gain*3 only"). For the Bi-fiber laser at 1160 nm (Fig. 14c), the fiber Raman gain is approximately 2 times lower than for the laser at 1150 nm, and the Raman contribution to the output power is also lower. Apparently, the simulation model with Raman gain as well as without it can be used for the 1160 nm laser description (compare Figs. 4b and 14c). The 1215 nm Bi-fiber laser was simulated using the energy-level scheme shown in Fig. 14, inset ***B***. At the wavelength of 1215 nm the fiber Raman gain coefficient is ~3 times lower than for 1160 nm laser. The results of the simulation are in a satisfactory agreement with the experiment (compare Figs. 4d and 14d).

Thus, operation of the Bi-fiber laser can be described using different simple energy-level schemes (Fig. 14) for different lasing wavelengths. A more adequate energy level scheme is necessary to combine the properties of the schemes mentioned above and to explain the observed temperature dependences.

6. CONCLUSION

In conclusion, we have studied the properties of high-power cw Bi-fiber lasers operating in the wavelength band of 1150–1215 nm. It was shown that Bi-fiber lasers can generate radiation powers of more than 15 W with the optical-to-optical efficiency of about 22% in the vicinity of 1160 nm. Saturation of the output power of the Bi fiber laser at a ≈5 W level was observed at a wavelength of 1215 nm. Unsaturable optical losses in Bi-doped fibers of approximately one-third of the total Bi-induced absorption were revealed. The temperature dependence of these losses in the region 0–60 °C and its influence on the efficiency of the Bi-fiber laser operation was investigated. It was demonstrated that two- and three-level schemes can be used for Bi-laser modeling in special cases of the laser generating at 1150–1160 nm and at 1215 nm. The possibility of yellow-light generation using a Bi-fiber laser was demonstrated. The main problems of Bi-doped fiber lasers at the current technology level are, apparently, large unsaturable optical losses and a low concentration of Bi ions in the fiber core. Solving these problems can enable one to develop efficient double-clad Bi-doped fibers.

ACKNOWLEDGMENTS

We thank V. M. Mashinsky, V. V. Dvoyrin, and A. L. Tomashuk (Fiber Optics Research Center of the Russian Academy of Sciences) and A. A. Umnikov, M. V. Yashkov, and A. N. Guryanov (Institute of Chemistry of High-Purity Substances of the Russian Academy of Sciences) for fruitful discussions and for help in the experiments.

REFERENCES

1. E. M. Dianov, I. A. Bufetov, V. M. Mashinsky, A. V. Shubin, O. I. Medvedkov, A. E. Rakitin, M. A. Melkumov, V. F. Khopin, and A. N. Guryanov, "Raman fiber lasers based on heavily GeO_2-doped fibers," Quantum Electron. **35**, 435–441 (2005).
2. E. Desurvire, "Optical communications in 2025," in *Proceedings of the 31st European Conference on Optical Communication* (ECOC, 2005) Vol. 1, pp. 5–6.
3. C. F. Blodi, S. R. Russell, J. S. Padilo, and J. C. Folk, "Direct and feeder vessel photocoagulation of retinal angiograms with dye yellow laser," Ophthalmology **6**, 791–795 (1990).
4. N. S. Sadick and R. Weiss, "The utilization of a new yellow light laser (578 nm) for the treatment of class I red telangiectasia of the lower extremities," J. Dermatol. Surg. **28**, 21–23 (2002).
5. C. E. Max, S. S. Olivier, H. W. Friedman, J. An, K. Avicola, B. V. Beeman, H. D. Bissinger, J. M. Brase, G. V. Erbert, D. T. Gavel, K. Kanz, M. C. Liu, B. Macintosh, K. P. Neeb, J. Patience, and K. E. Waltjen, "Image improvement from a sodium-layer laser guide star adaptive optics system," Science **277**, 1649–1651 (1977).
6. Y. Fujimoto and M. Nakatsuka, "Infrared luminescence from bismuth-doped silica glass," Jpn. J. Appl. Phys. **40**, L279–L281 (2001).
7. M. Peng, J. Qiu, D. Chen, X. Meng, I. Yang, X. Jiang, and C. Zhu, "Bismuth- and aluminum-codoped germanium oxide glasses for super-broadband optical amplification," Opt. Lett. **29**, 1998–2000 (2004).
8. X. Meng, J. Qiu, M. Peng, D. Chen, Q. Zhao, X. Jiang, and C. Zhu, "Near infrared broadband emission of bismuth-doped aluminophosphate glass," Opt. Express **13**, 1628–1634 (2005).
9. X. Meng, J. Qiu, M. Peng, D. Chen, Q. Zhao, X. Jiang, and C. Zhu, "Infrared broadband emission of bismuth-doped barium-aluminum-borate glasses," Opt. Express **13**, 1635–1642 (2005).
10. V. V. Dvoyrin, V. M. Mashinsky, E. M. Dianov, A. A. Umnikov, M. V. Yashkov, and A. N. Guryanov, "Absorption, fluorescence and optical amplification in MCVD bismuth-doped silica glass optical fibres," in *Proceedings of the 31st European Conference on Optical Communication* (ECOC, 2005) Vol. 4, pp. 949–950.
11. E. M. Dianov, V. V. Dvoyrin, V. M. Mashinsky, A. A. Umnikov, M. V. Yashkov, and A. N. Guryanov, "CW bismuth fibre laser," Quantum Electron. **35**, 1083–1084 (2005).
12. V. V. Dvoyrin, V. M. Mashinsky, L. I. Bulatov, I. A. Bufetov, A. V. Shubin, M. A. Melkumov, E. M. Dianov, A. A. Umnikov, V. F. Khopin, M. V. Yashkov, and A. N. Guryanov,

"Bismuth-doped-glass optical fibers - a new active medium for lasers and amplifiers," Opt. Lett. **31**, 2966–2968 (2006).
13. R. Paschotta, J. Nilsson, A. C. Tropper, and D. C. Hanna, "Ytterbium-doped fiber amplifiers," IEEE J. Quantum Electron. **33**, 1049–1056 (1997).
14. V. V. Dvoyrin, V. M. Mashinsky, E. M. Dianov, A. A. Umnikov, M. V. Yashkov, and A. N. Guryanov, "Bi-doped silica fibers - a new active medium for tunable fiber lasers and broadband fiber amplifiers," in *Optical Fiber Communication Conference and the National Fiber Optic Engineers Conference*, on CD-ROM (Optical Society of America, 2006), paper OTuH4.